

Radial diffusion model for fragrance materials: prediction and validation

Rafael N. Almeida^{a}, Alírio E. Rodrigues^b, Rubem M. F. Vargas^a, Eduardo Cassel^a*

^aUnit Operations Lab, Polytechnic School, Pontifical Catholic University of Rio Grande do Sul, Av. Ipiranga 6681 - Prédio 30, Bloco F, Sala 208, Porto Alegre, Brazil

^bLSRE-Laboratory of Separation and Reaction Engineering, Associate Laboratory LSRE/LCM, Faculdade de Engenharia, Universidade do Porto, Rua Dr. Roberto Frias, 4200-465, Porto, Portugal

*Corresponding author: Rafael N. Almeida. E-mail: r.nolibos@edu.pucrs.br Tel.: +55 51 3353 4585.

Topical Heading: Transport Phenomena and Fluid Mechanics

Keywords: evaporation, perfume, Fick's second law, headspace, mathematical modelling

Abstract

A predictive model based on Fick's second law for radial diffusion is proposed and validated for modeling the diffusion of fragrances. A pure component, two binary systems, and a ternary system were used for validation. The model combines the prediction model to represent the liquid phase non-idealities, using the UNIFAC group contribution method, with the Fickian radial diffusion approach. The experimental headspace concentrations were measured in a diffusion chamber using the solid-phase microextraction (SPME) technique and quantified using gas chromatography with a flame ionization detector (GC-FID). The numerical solutions were obtained along with an analytical model considering constant surface concentration. The odor intensities of

the studied systems were calculated using Stevens' power law and the strongest component model, respectively. The numerical simulation presented good adherence to the experimental gas concentration data. The proposed methodology is an efficient and validated tool to assess the radial diffusion of fragrance and volatile systems.

1. INTRODUCTION

Odor can be a significant environmental parameter since it can be related to the human perception of comfort and to the sanitary conditions of an indoor atmosphere.¹ Fragrance materials and volatile organic compounds are common ingredients of a large number of products (perfumes, cosmetics, household cleaners, or detergents) due to their odorant capacity and attractiveness to consumers. Olfactory marketing is a growing trend, using scents to stimulate shopping, adding competitive advantage, and creating a deeper connection with the brand and the physical sales space.² The formulation process of fragrances is mainly a costly trial-and-error process that involves testing hundreds of mixtures until the desired scent is reached³. In this context, product engineering has been used to introduce some thermodynamics and mass transfer knowledge into an empirical and experimental area.⁴ Through the use of scientific principles, it has been possible to predict the odor behavior of complex fragrance mixtures through their liquid composition, using psychophysical parameters (such as odor threshold and power-law exponent).⁵

The diffusion of perfumes and fragrances in the air has been recently the object of study through a differential mass transfer approach.^{4,6–8} The thermodynamics is well-described by the available methods and one-dimensional (1-D) mass transfer models

were proposed and validated.^{9,10} However, as the propagation of a fragrance occurs in all directions, a more realistic description of the phenomenon is achieved with a three-dimensional representation. Two recent theoretical approaches were proposed: the first regarding cartesian coordinates¹¹ and the latter from a theoretical radial perspective³. Pereira et al.¹¹ focused on the trail of perfumes, analyzing its diffusion from a moving source, with 1-D validation. Pereira et al.³ presented a theoretical radial model for the fragrance diffusion, based on a numerical correlation to the cartesian one-dimensional model. The gas-tight syringe sampling method (used for 1-D validation) is not suitable for open space as the radial perspective demands, thus the development of methodologies for the quantification of volatile compounds is required.

Among headspace sampling techniques, headspace solid-phase microextraction (HS-SPME) has specific advantages over conventional static, dynamic, and purge and trap techniques: it is economic, faster, and requires little manipulation of samples.¹² The HS-SPME method was introduced in 1990,¹³ and it has gained increasing popularity for fragrance analysis, especially as an alternative to dynamic headspace methods. It is especially suitable for qualitative and quantitative analyses of fragrance compounds released by fragrant samples, since SPME provides linear results over a wide concentration range, often down to parts per trillion.¹⁴

The HS-SPME is a solvent-free sampling technique in which the analytes from the liquid or gaseous sample are directly absorbed or adsorbed (or both) onto a polymer-coated fused silica fiber, which is part of the needle of a specially designed holder.¹⁵ The sampled analytes can be recovered either by thermal desorption directly into a GC injection port or by solvent elution into a modified high-performance liquid

chromatographic (HPLC) injection valve. The state of the art concerning SPME theory, technology, evolution, applications, and specific topics have been reviewed by Pawliszyn et al.^{16–18} The amount of analyte concentrated through HS-SPME in a fiber is the result of two distinct equilibria: the first is the matrix/HS equilibrium, and the second is the HS/polymeric fiber coating equilibrium. The total HS-SPME recovery of an analyte from a solid or liquid matrix depends on the overall partition coefficient of the analyte between the SPME fiber coating and the matrix itself.¹⁹ For the case of fragrance and flavor compounds, the International Organization of the Flavor Industry presents HS-SPME guidelines for the use of SPME for quantitative analysis.²⁰

Therefore, using the technique of HS-SPME, a sampling methodology was developed to validate the radial diffusion model. For this purpose, the radial diffusion of perfume raw materials (PRMs) and a simple ethanolic mixture were evaluated. Their gas concentrations were experimentally measured inside a closed chamber and analyzed using gas chromatography with a flame ionization detector (GC-FID). The headspace profiles were converted into perceived odor using the psychophysical model Stevens' power law,²¹ and the odor character was assessed by the strongest component model. The numerical solutions were obtained using MATLAB routines. Finally, the predicted results by the numerical simulation were compared with the experimental data.

2. MATERIALS AND METHODS

2.1. Chemicals

Eucalyptol (1,8-cineole) (CAS No. 470-82-6, purity $\geq 99\%$) and (R)-(+)-limonene (CAS No. 5989-27-5, purity 97 %) were obtained from Sigma-Aldrich. Ethanol (CAS No. 64-17-5, purity $\geq 99.5\%$) was obtained from Merck. All reagents were used as received without further purification. **Table 1** presents some relevant physicochemical properties of these components.

Table 1. Properties of the perfume raw materials: molecular formula, molecular weight (MW), vapor pressure (P_i^{sat}) at 25 °C, molecular diffusivity in air ($D_{i,air}$), odor detection threshold (ODT), power law exponent (m_i).

Compound	Molecular formula ^a	MW (g/mol) ^a	P_i^{sat} (Pa) ^b	$D_{i,air} \times 10^2$ (m ² /h) ^c	ODT _i ^d	m_i ^e
Eucalyptol	C ₁₀ H ₁₈ O	154.25	253.4	2.17	5.60E-04	0.39
Limonene	C ₁₀ H ₁₆	136.23	192.0	2.17	1.22E-05	0.37
Ethanol	C ₂ H ₆ O	46.10	7050	4.42	1.03E-02	0.58

^aFrom PubMed.gov, U.S. National Library of Medicine National Institutes of Health.

^bExperimental values from PubChem Database.²² ^cEstimated from Fuller et al.²³. ^dODTs (defined odor detection thresholds) were geometrically averaged from data available in van Gemert.²⁴ ^eFrom Devos et al.²⁵.

2.2. Experimental design

A special chamber, consisting of closed walls and opened top, was developed for the headspace sampling (**Figure 1**). Inside the chamber, three HS-SPME holders were placed at different cartesian positions, but at the same distance from the diffusion source. Samples were collected over time, in triplicate, at 10, 15, 20, 30 and 40 cm distances from the source, being placed at random cartesian positions in order to evaluate system isotropy. The sampling times were 15, 30, 60 and 120 min.

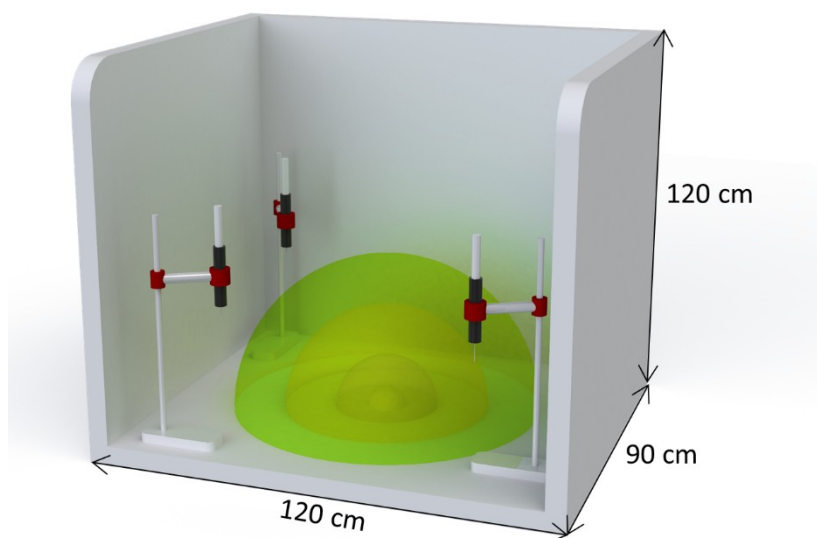


Figure 1. Diffusion chamber scheme (side window for visualization).

The liquid samples (2 mL) of the perfume raw materials (PRMs) were placed in a small cap with 1.5 cm diameter at the chamber center. The chamber was placed inside a bigger closed room in order that no air disturbance could alter the diffusion profile. Room temperature was monitored, and the experiments were conducted at 23.5 ± 0.6 °C. At first, the pure component (PC) diffusion was evaluated, followed by two binary systems composed by a PRM and ethanol (BS1 and BS2), and finally a ternary system (TS) was evaluated with the two top notes and the solvent (ethanol), as demonstrated in Table 2. The mole fractions were obtained from 1:2 solutions for the binary systems and 1:1:2 solutions for ternary system.

Table 2. Mole fractions (x_i) of each component in the studied fragrance systems.

Fragrance component	x_i			
	PC	BS1	BS2	TS
Eucalyptol	1.000	0.149	–	0.131
Limonene	–	–	0.140	0.121
Ethanol	–	0.851	0.860	0.748

A 2-cm dual-layered SPME fiber coated with highly crosslinked 50/30- μm divinylbenzene/Carboxen, each suspended in polydimethylsiloxane (DVB/CAR/PDMS) (Supelco, Bellefonte, PA), was used for the headspace sampling. The syringe holder device (Supelco) with the fiber was conditioned before each use at 250 °C for 30 min in a GC injector, as recommended by the manufacturer. The conditions for HS-SPME of the calibration curves were as follows: sample amount, 2 mL of each pure PRM; vial volume, 15 mL; equilibration and sampling time, 60 min at 25 °C; split mode varying from 10, 50, 100, 200, 300 to 500.

The diffusion samples were then analyzed using an Agilent 7890A gas chromatograph (Agilent Technologies, USA). The injector used was in splitless mode at 250 °C. The capillary column used was a HP-5MS (30 m x 250 μm i.d., 0.25 μm phase thickness, Agilent Technologies, USA), coated with 5% phenyl methyl silane. The oven temperature started at 60 °C, raised to 250 °C at 20 °C min^{-1} , then held for 2 min. Carrier gas was Helium with a flow rate of 1 mL min^{-1} . The FID detector was maintained at 250 °C.

2.3. Mathematical model

The radial diffusion predictive model considers that the diffusion of odorants occurs in all directions and at the same diffusion rate regardless of the direction the component is diffusing in (isotropic), in this way, extending the concentration profiles to a three-dimensional case.²⁶

The diffusion source point is considered to be the gas control volume origin. The radial diffusion model is based on Fick's second law for radial diffusion, in order to evaluate the transient diffusion where the variable r represents the distance from the

source. The equilibrium concentration is obtained through the Raoult's modified law and the activity coefficient with UNIFAC. For the gas phase mass balance:

$$\frac{\partial y_i}{\partial t} = D_{i-mix} \left(\frac{2}{r} \frac{\partial y_i}{\partial r} + \frac{\partial^2 y_i}{\partial r^2} \right) \quad (1)$$

where y_i is the mole fraction of component i in the headspace gas as a function of distance r from the source and time t , D_{i-mix} is the diffusivity coefficient of each component i in headspace mixture. The initial condition ($t=0$) is:

$$y_i(r, 0) = y_{i,0} = 0 \quad (2)$$

The equilibrium at the gas/liquid interface at the diffusion source point ($r=0$), and the boundary condition at $r=R_{max}$:

$$y_i(0, t) = y_{i,eq} = \frac{\gamma_i P_i^{sat} x_i}{P} \quad (3)$$

$$\frac{\partial y_i(R_{max}, t)}{\partial r} = 0 \quad (4)$$

where, γ_i is the activity coefficient of component i , P_i^{sat} is the vapor pressure of component i , P is the system pressure and R_{max} is the maximum distance in the radial coordinate. x_i is the mole fraction of the component i in the liquid phase, experimentally obtained by $x_i = n_i / n_T$ where n_i is the number of moles of component i in the liquid phase and n_T is the total number of mols in the liquid phase. The activity coefficients were obtained for each of the numerical iterations performed throughout the solution of the model; the UNIFAC method²⁷ is included in the routine, in this way, varying along with the liquid composition. The headspace gas concentration is then obtained from the following relation:

$$c_i^g = y_i c_T = \frac{y_i MW_i P}{RT} \quad (5)$$

where MW_i is the molecular weight of component i , R is the universal gas constant and T is the system temperature. The mass balance at the liquid phase is given by the following ordinary differential equation (ODE):

$$\frac{\partial n_i}{\partial t} = -D_{i-mix} A_{lg} \frac{P}{RT} \frac{\partial y_i}{\partial r} \Big|_{r=0} \quad (6)$$

where n_i is the number of moles of component i in the liquid phase. The liquid phase was considered a nonideal mixture and its composition changes during the evaporation of the fragrance through the liquid-gas (A_{lg}) interface. The initial condition to the liquid phase is $n_i(0) = n_{i,0}$, which is determined for each component based on its specific mass, volume, and molecular weight.

The partial differential equations system was computed in MATLAB, using the method of lines for discretization and the ODEs solved with the `ode15s` package with 10^{-8} tolerance. This method is a variable-step; variable-order (VSVO) solver based on the numerical differentiation formulas (NDFs) of orders 1 to 5 and suited for stiff problems.

Another approach is possible considering a source continuously releasing fragrance in a semi-infinite medium, at a constant concentration at the surface and gas-liquid interface. Which is valid in the case of a large liquid volume, since the evaporation rate does not alter the liquid phase global composition (opened perfume bottle, or a fragrance diffuser with a large volume) and valid for short intervals of time. This approach is also valid for a pure substance diffusion. From Fick's second law and considering only radial diffusion:

$$\frac{\partial c_i^g}{\partial t} = D_{i-mix} \nabla^2 c_i^g = \frac{D_{i-mix}}{r^2} \frac{\partial}{\partial r} \left(r^2 \frac{\partial c_i^g}{\partial r} \right) \quad (7)$$

The solution obtained from Equation 7, that represents the radial diffusion model, submitted to $c_i^g(0, r) = 0$, $c_i^g(t, R_s) = c_{i,eq}$ and $c_i^g(t, \infty) = 0$ is as follows²⁶:

$$c_i^g(t, r) = \frac{c_{i,eq} R_s}{r} \operatorname{erfc} \left(\frac{r - R_s}{2 \sqrt{D_{i-mix} t}} \right) \quad (8)$$

where $c_{i,eq} = \gamma_i P_i^{sat} MW_i x_i / RT$ is the equilibrium concentration at the gas-liquid interface and R_s is the source radius.

2.4. Odor intensity

The intensity of a fragrance material can then be expressed in terms of its odor intensity (ψ) through the psychophysical model Stevens' power law, by its definition²¹:

$$\psi_i = \left(\frac{c_i^g}{ODT_i} \right)^{m_i} \quad (9)$$

where ODT_i is the odor threshold concentration of component i in the air. ODTs geometric mean values were calculated in order to minimize variabilities between data collected from the van Gemert²⁴ database.

The concept of odor intensity was created in order to assist in the formulation of perfumes, in order to identify, from the composition of the liquid mixture, the characteristic odor of the perfume.²⁸ The ψ is calculated individually for each component of the mixture and the maximum odor value is determined from the total set:

$$\psi_{max} = \max (\psi_A, \psi_B, \psi_C, \dots, \psi_i) \quad (10)$$

3. RESULTS AND DISCUSSION

The radial diffusion experiments were performed and compared to the predictive model used to simulate the evaporation behavior of pure and multicomponent perfume liquid mixtures. The two binary systems were composed by a top note (eucalyptol or limonene) and ethanol. In the case of ternary mixtures, two top notes (eucalyptol and limonene) were used in addition to the solvent (ethanol). The systems were composed by high volatility compounds due to the experimental technique applied (SPME). The sampling times were defined based on the fiber saturation point. As expected, it was observed that after longer interval times, the quantified sample no longer varies linearly with the headspace concentration.

3.1. Pure component diffusion

The experimental headspace concentrations for eucalyptol were obtained at five fixed positions (SP1 = 10 cm, SP2 = 15 cm, SP3 = 20 cm, SP4 = 30 cm, and SP5 = 40 cm) using the conditions described before (see the Experimental design section). Figure 2. presents the experimental data compared with those obtained using the theoretical model to predict the radial diffusion of PRMs. The proposed model fits well with the experimental data. As expected, different headspace concentrations were found depending on the distance from the source, as the headspace concentrations are higher for distances closer to the scented source. The analytical solution of the proposed mathematical model for pure compounds or large liquid volumes were also applied to the experimental data and is represented in Figure 2.. For short diffusion times it is possible to notice that the analytical solution and the numerical solution overlap since

that in the first moments the initial liquid concentration has not yet been changed. The analytical solution has a computational cost much lower than the numerical one, and therefore, it should be applied whenever possible. This solution is valid when the equilibrium concentration at the liquid-vapor interface remains constant throughout the evaporation process.

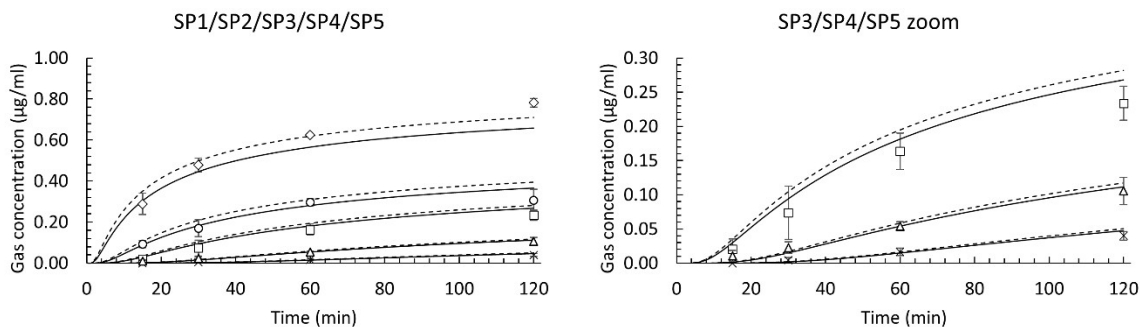


Figure 2. Headspace concentration profiles at 23.5 °C for pure component eucalyptol in air at different distances from the source. Experimental radial concentration at (◇) SP1, (○) SP2, (□) SP3, (△) SP4 and (x) SP5, (—) radial model numerical solution and (- - -) radial analytical solution.

In order to assess the analytical model performance for short times, the mean absolute error (MAE) for the first 5 minutes of diffusion between the two models was calculated, and at the 10 cm distance is $MAE_{5,10} = 0.01142 \mu\text{g/ml}$ and for the last 5 minutes (115 to 120 minutes) is $MAE_{115,10} = 0.0622 \mu\text{g/ml}$. Following the same logic, $MAE_{5,20} = 0.0011 \mu\text{g/ml}$ and $MAE_{115,20} = 0.02517 \mu\text{g/ml}$, showing that the greater the distance from the source, the smaller the error, regardless of the time interval evaluated. Evaluating within the same distance from the source, errors are much smaller in the first moments of diffusion, as expected since there is no considerable variation in composition in the liquid phase.

3.2. Binary systems

Considering the diffusion of eucalyptol in ethanolic mixture (BS1), the predicted and experimental headspace concentrations evaluated at two different distances from the liquid source (SP1 – 10 cm and SP3 – 30 cm) are presented in Figure 3. It is also presented in Figure 4 the concentration profiles for the system limonene/ethanol (BS2) at the same distance than BS1. In the same way as the pure component experiment, the simulation of BS1 and BS2 fit well with the experimental data.

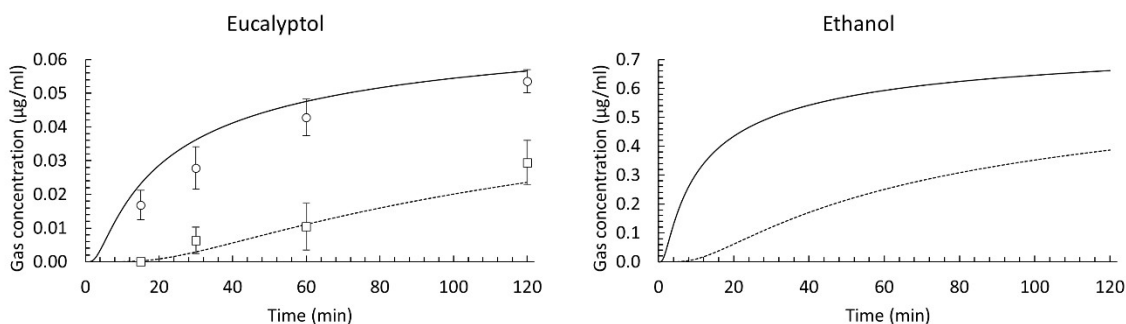


Figure 3. Headspace concentration profiles for binary mixture BS1 (eucalyptol/ethanol) at 23.5 °C in air at different distances from the source. (○) Eucalyptol experimental concentration at 10 cm and (□) at 30 cm from the source, (—) radial model numerical solution at 10 cm and (- -) at 30 cm from the source.

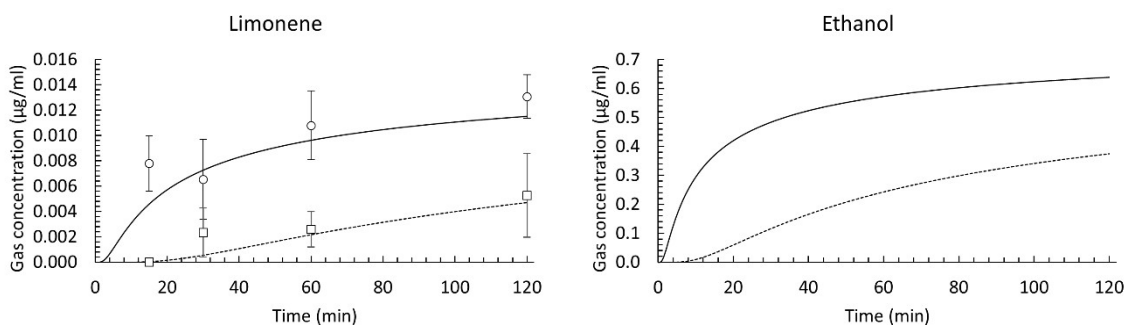


Figure 4. Headspace concentration profiles for binary mixture BS2 (limonene/ethanol) at 23.5 °C in air at different distances from the source. (○) Limonene experimental concentration at 10 cm and (□) at 30 cm from the source, (—) radial model numerical solution at 10 cm and (- -) at 30 cm from the source.

The differences in the headspace concentration of the two compounds when in ethanolic solution are remarkable; since the initial mole fractions are similar, and the diffusivities and the vapor pressure values are alike as well (253 Pa and 192 Pa). If the liquid phases were to be considered ideal, this effect would not be predicted by the model and the volumetric/energetic interactions between PRM and the solvent would be neglected. In this case, the two substances present similar structures sizes but the eucalyptol molecule has an oxygenated function (ether).

3.3. Ternary system

A ternary system (TS) was studied in order to evaluate the liquid phase interactions. Perfumes are a much more complex system than the one presented, but the two top note components were selected to validate the predictive model, since its volatilities guarantee the minimum headspace concentration in which the SPME technique is still reliable. The system is composed by a volumetric ratio of 1:1:2 of eucalyptol/limonene/ethanol. Middle and bottom notes were not considered in the present study since their experimental headspace concentrations are very low and difficult to quantify with accuracy using GC-FID. However, it seems reasonable to extrapolate that the model would predict the behavior of these notes, since the simulation for the two molecules was validated by the experimental data. From Figure 5 it can be observed that the model is able to predict the headspace concentrations of eucalyptol and limonene. As seen for the binary systems, eucalyptol presents higher headspace concentrations than limonene, and concentrations decreased as the distance from the source increased.

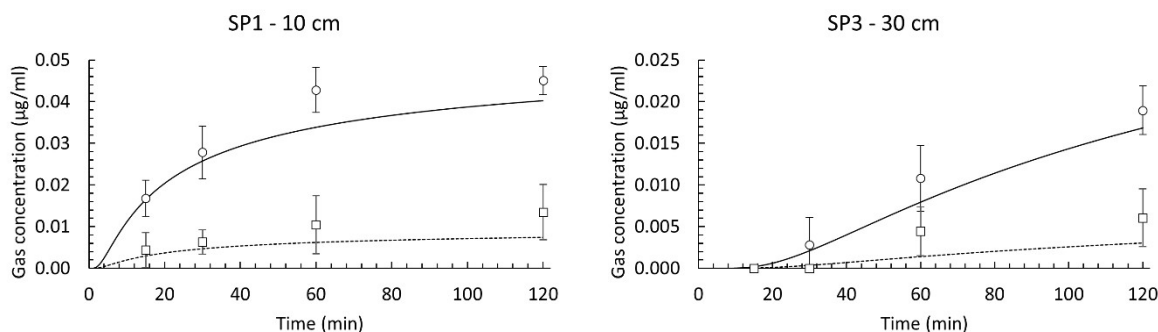


Figure 5. Headspace concentration profiles for ternary mixture TS (eucalyptol/limonene/ethanol) at 23.5 °C in air at different distances from the source. (○) Eucalyptol experimental concentration, (□) limonene experimental concentration, radial model numerical solution for (—) eucalyptol and (---) limonene.

The ternary results also exposed influence of the liquid composition on the two top notes equilibrium (eucalyptol and limonene); comparing both binaries (Figure 3 and Figure 4) and ternary (Figure 5) fragrance systems, a decrease in the headspace concentrations of eucalyptol and limonene is notable, suggesting that the interactions in the liquid phase have an important contribution to the composition of the vapor phase, since the two molecules are more retained in the liquid phase (even with the same initial number of moles in the mixture). As suggested by the experimental results and predicted by the model, further distances from the source present a more linear gas concentration profile, which simplifies the phenomena representation at longer times and larger spaces.

For the TS mixture, the predicted headspace concentrations were converted into odor perceptions using the Stevens' power law model (Figure 6). The odor profiles of the ternary system were calculated using the simulated and validated headspace concentrations, except for the ethanol experimental values which required a different experimental design (fiber and GC method).

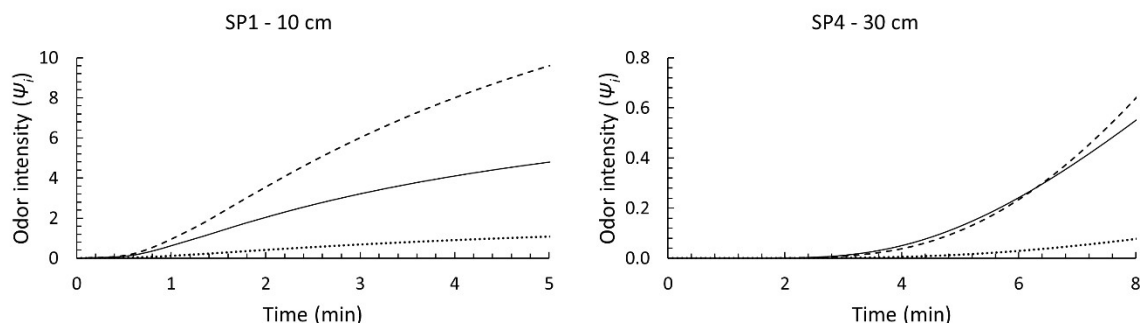


Figure 6. Predicted odor intensities of the ternary fragrance mixture at two different distances (SP1 and SP4) minutes after release. (– –) Eucalyptol, (—) ethanol and (.....) limonene.

At the closest evaluated distances, the odor intensities profiles follow the same trend as the equilibrium concentration and ODT ratio; even though ethanol is almost 30 times more volatile than eucalyptol, the different ODT values cause the strongest component to be the eucalyptol at 10 cm from the source. For a slightly larger distance from the source, the model describes a higher ethanol odor intensity in the first minutes, a recurrent sensation when opening a perfume bottle or moments after applying it. In addition to its high volatility, ethanol diffuses twice as fast as other molecules due to its smaller molecular size.

4. CONCLUSIONS

The proposed experimental methodology was validated using a diffusion chamber, a high-capacity concentration technique and evaluating the perfume raw materials concentration profiles for different distances from the source. The predicted profiles agreed with the experimental diffusion profiles, even inside the limited experimental range available for validation (short time interval due to fiber saturation and specific top notes due to low concentrations of lower volatility notes). The

experimental challenge was to evaluate the diffusion of a PRM/ethanol mixture, and observing the experimental validation limits, two top notes (eucalyptol and limonene) were used in order to investigate the liquid phase non-idealities. The ternary headspace concentration profiles were compared to those of the pure component profiles and the influence of the liquid compositions on the gas phase profiles and respective odor intensities were confirmed. These results are as expected since there are molecular interactions between the PRMs in the liquid phase. In this way, the proposed model can efficiently predict the radial diffusion of perfume raw materials and their multicomponent mixtures. The proposed radial predictive model is a much more realistic phenomenon description, it provides relevant information over time and distance and it can also be used for other volatile organic compounds (VOCs) of interest, under the same scenario.

Acknowledgment

The present work was carried out with the support of CNPq, National Council of Scientific and Technological Development and CAPES, Coordination of Superior Level Staff Improvement.

References

1. Augusto F, Lopes AL, Zini CA. Sampling and sample preparation for analysis of aromas and fragrances. *TrAC Trends Anal Chem.* 2003;22(3):160-169.
2. Spangenberg ER, Crowley AE, Henderson PW. Improving the store environment: do olfactory cues affect evaluations and behaviors? *J Mark.* 1996;60(2):67-80.
3. Pereira J, Costa P, Loureiro JM, Rodrigues AE. Modelling diffusion of fragrances: A radial perspective. *Can J Chem Eng.* 2019;97(1):351-360.

4. Teixeira MA, Rodriguez O, Gomes P, Mata V, Rodrigues A. *Perfume Engineering: Design, Performance and Classification*. Butterworth-Heinemann; 2012.
5. Costa P, Teixeira MA, Lièvre Y, Loureiro JM, Rodrigues AE. Modeling Fragrance Components Release from a Simplified Matrix Used in Toiletries and Household Products. *Ind Eng Chem Res*. 2015;54(46):11720-11731.
6. Teixeira MA, Rodríguez O, Mata VG, Rodrigues AE. The diffusion of perfume mixtures and the odor performance. *Chem Eng Sci*. 2009;64(11):2570-2589.
7. Almeida RN, Costa P, Pereira J, Cassel E, Rodrigues AE. Evaporation and Permeation of Fragrance Applied to the Skin. *Ind Eng Chem Res*. 2019;58(22):9644-9650.
8. Teixeira MA, Rodríguez O, Rodrigues AE. Diffusion and performance of fragranced products: Prediction and validation. *AIChE J*. 2013;59(10):3943-3957.
9. Mata VG, Gomes PB, Rodrigues AE. Effect of Nonidealities in Perfume Mixtures Using the Perfumery Ternary Diagrams (PTD) Concept. *Ind Eng Chem Res*. 2005;44(12):4435-4441.
10. Teixeira MA, Rodríguez O, Mota FL, Macedo EA, Rodrigues AE. Evaluation of Group-Contribution Methods To Predict VLE and Odor Intensity of Fragrances. *Ind Eng Chem Res*. 2011;50(15):9390-9402.
11. Pereira J, Costa P, Coimbra MC, Rodrigues AE. The trail of perfumes. *AIChE J*. 2018;00(00):1-8.
12. Pawliszyn J. *Solid Phase Microextraction: Theory and Practice*. John Wiley & Sons; 1997.
13. Arthur CL, Pawliszyn J. Solid phase microextraction with thermal desorption using

- fused silica optical fibers. *Anal Chem.* 1990;62(19):2145-2148.
14. Knupp G, Kusch P, Neugebauer M. Identification of flavor components in perfumes by headspace solid-phase microextraction and gas chromatography-mass spectrometry. *J Chem Educ.* 2002;79(1):98.
 15. Zhang Z, Pawliszyn J. Headspace solid-phase microextraction. *Anal Chem.* 1993;65(14):1843-1852.
 16. Souza-Silva ÉA, Gionfriddo E, Pawliszyn J. A critical review of the state of the art of solid-phase microextraction of complex matrices II. Food analysis. *TrAC Trends Anal Chem.* 2015;71:236-248.
 17. Lord H, Pawliszyn J. Evolution of solid-phase microextraction technology. *J Chromatogr A.* 2000;885(1-2):153-193.
 18. Souza-Silva ÉA, Jiang R, Rodríguez-Lafuente A, Gionfriddo E, Pawliszyn J. A critical review of the state of the art of solid-phase microextraction of complex matrices I. Environmental analysis. *TrAC Trends Anal Chem.* 2015;71:224-235.
 19. Bicchi C, Cordero C, Rubiolo P. A survey on high-concentration-capability headspace sampling techniques in the analysis of flavors and fragrances. *J Chromatogr Sci.* 2004;42(8):402-409.
 20. Analysis IWG on M of. Guidelines for solid-phase micro-extraction (SPME) of volatile flavour compounds for gas-chromatographic analysis, from the Working Group on Methods of Analysis of the International Organization of the Flavor Industry (IOFI). *Flavour Fragr J.* 2010;25(6):404-406.
 21. Stevens SS. On the psychophysical law. *Psychol Rev.* 1957;64(3):153.
 22. Kim S, Chen J, Cheng T, et al. PubChem 2019 update: improved access to

- chemical data. *Nucleic Acids Res.* 2019;47(D1):D1102-D1109.
23. Fuller EN, Schettler PD, Giddings JC. New method for prediction of binary gas-phase diffusion coefficients. *Ind Eng Chem.* 1966;58(5):18-27.
 24. Van Gemert LJ. Compilations of odour threshold values in air, water and other media. Published online 2003.
 25. Devos M. *Standardized Human Olfactory Thresholds*. Oxford University Press, USA; 1990.
 26. Crank J. *The Mathematics of Diffusion*. Oxford university press; 1979.
 27. Fredenslund A. *Vapor-Liquid Equilibria Using UNIFAC: A Group-Contribution Method*. Elsevier; 2012.
 28. Teixeira MA, Barrault L, Rodríguez O, Carvalho CC, Rodrigues AE. Perfumery Radar 2.0: A Step toward Fragrance Design and Classification. *Ind Eng Chem Res.* 2014;53(21):8890-8912.